ORGANIC LETTERS

2010
Vol. 12, No. 20
4520−4523

Synthesis of π-Extended Thiadiazole (Oxides) and Their Electronic Properties

Thomas Linder, Eider Badiola, Thomas Baumgartner,* and Todd C. Sutherland*

Department of Chemistry, University of Calgary, 2500 University Drive NW, Calgary, Alberta, Canada T2N 1N4

thomas.baumgartner@ucalgary.ca; todd.sutherland@ucalgary.ca

Received August 4, 2010

ABSTRACT

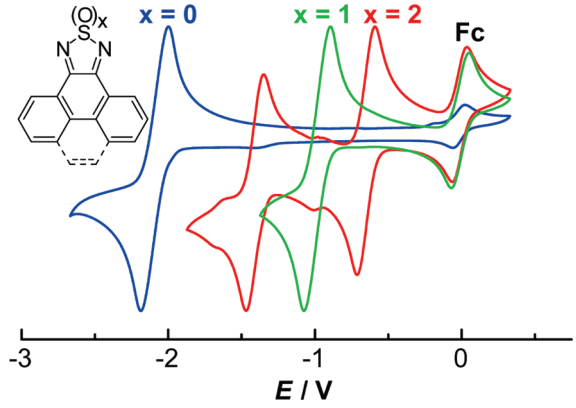

The syntheses of extended thiadiazole, thiadiazole oxide, and thiadiazole dioxide heterocycles are described. The electron-accepting heterocycles were investigated by X-ray crystallography and optical as well as electrochemical measurements and supported by DFT calculations. The thiadiazole dioxide heterocycles have reduction potentials of −0.7 V vs ferrocene/ferrocenium, suggesting a viable building block for *n*-type organic materials.

Conjugated polymers and oligomers[1] have shown utility in organic electronic applications, such as organic light-emitting diodes (OLEDs),[2] organic field effect transistors (OFETs),[3] and organic photovoltaics (OPVs).[4] Several hole-transporting (*p*-type) polymers show competitive conductivities with inorganic analogues; however, there are only few examples of electron-transporting (*n*-type) polymers.[5]

The limited number of organic *n*-type materials is due to the availability of monomers with low-lying LUMO energy levels. Representative *n*-type building blocks include benzothiadiazole (BTD),[6] perylene bisimide,[7] and PCBM (phenyl-C_{61}-butyric acid methyl ester).[8] A common theme in the design of new *n*-type species is the incorporation of fused heterocycles into the materials' backbone. BTD has been utilized in a variety of copolymers because of its *n*-type character, synthetic access, and lower cost. To date, BTD has been an essential acceptor component in the design of donor polymers for bulk

(1) (a) Brédas, J.-L.; Beljonne, D.; Coropceanu, V.; Cornil, J. *Chem. Rev.* **2004**, *104*, 4971–5003. (b) Günes, S.; Neugebauer, H.; Sariciftci, N. S. *Chem. Rev.* **2007**, *107*, 1324–1338. (c) Heeger, A. J. *Synth. Met.* **2001**, *125*, 23–42. (d) Roncali, J.; Blanchard, P.; Frère, P. *J. Mater. Chem.* **2005**, *15*, 1589–1610.

(2) (a) Burn, P. L.; Lo, S.-C.; Samuel, I. D. W. *Adv. Mater.* **2007**, *19*, 1675–1688. (b) Hudson, Z. M.; Wang, S. *Acc. Chem. Res.* **2009**, *42*, 1584–1596. (c) Kivala, M.; Diederich, F. *Acc. Chem. Res.* **2009**, *42*, 235–248.

(3) (a) Allard, S.; Forster, M.; Souharce, B.; Thiem, H.; Scherf, U. *Angew. Chem., Int. Ed.* **2008**, *47*, 4070–4098. (b) Ortiz, R. P.; Facchetti, A.; Marks, T. J. *Chem. Rev.* **2010**, *110*, 205–239. (c) Shirota, Y.; Kageyama, H. *Chem. Rev.* **2007**, *107*, 953–1010. (d) Smith, J.; Hamilton, R.; McCulloch, I.; Stingelin-Stutzmann, N.; Heeney, M.; Bradley, D. D. C.; Anthopoulos, T. D. *J. Mater. Chem.* **2010**, *20*, 2562–2574.

(4) (a) Brédas, J.-L.; Durrant, J. R. *Acc. Chem. Res.* **2009**, *42*, 1689–1690. (b) Mishra, A.; Fischer, M. K. R.; Bäuerle, P. *Angew. Chem., Int. Ed.* **2009**, *48*, 2474–2499. (c) Roncali, J. *Acc. Chem. Res.* **2009**, *42*, 1719–1730. (d) Segura, J. L.; Martin, N.; Guldi, D. M. *Chem. Soc. Rev.* **2005**, *34*, 31–47. (e) Steim, R.; Kogler, F. R.; Brabec, C. J. *J. Mater. Chem.* **2010**, *20*, 2499–2512. (f) Winder, C.; Sariciftci, N. S. *J. Mater. Chem.* **2004**, *14*, 1077–1086.

10.1021/ol1018213
Published on Web 09/16/2010

heterojunction solar cells[9] because of its absorption properties, high mobilities, and excellent photovoltaic performance. However, the electron-accepting properties of BTD are only moderate, and more electron-deficient building blocks would enable access to LUMO tuning that could be incorporated into Donor−Acceptor (D−A) polymers. Lowering of the LUMO level through modification of the acceptor component in these D−A copolymers will enable improved light-harvesting characteristics, and adding fused aromatics should lead to a higher degree of crystallinity in the eventual polymer, which could provide superior charge-transport properties.

In this contribution, we explore two effects on the thiadiazole heterocycle: first, the consequence of changing the fused phenyl ring in BTD to either a phenanthrene or pyrene backbone and second, changing the oxidation state of the sulfur in the thiadiazole heterocycle from S(II) via S(IV) to S(VI).

The synthesis of six thiadiazoles begins with the phenanthryl and pyrenyl bis-imines **1a**,**b** (Scheme 1) that

Scheme 1. Synthesis of Thiadiazole Heterocycles

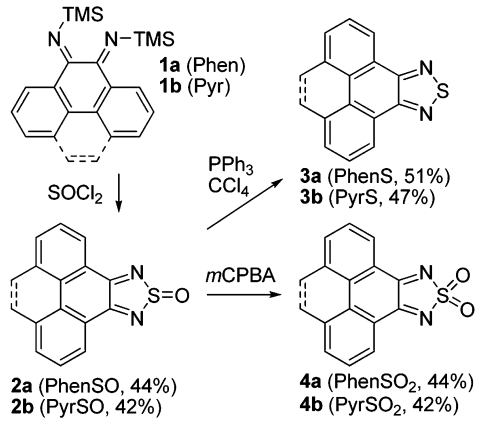

are accessible from the corresponding α-diketones. Each bis-imine was cleanly converted to the thiadiazole oxide heterocycle, **2a**,**b**, by addition of thionyl chloride in toluene. Heterocycles **2a**,**b** are further reduced with PPh_3 in CCl_4[10] to give thiadiazoles **3a**,**b** or, alternatively, oxidized with peroxy acid to give thiadiazole dioxides **4a**,**b**.[10b,11] Note that others have synthesized thiadiazole[12] and thiadiazole dioxide[13] heterocycles using different approaches. The advantage of the present method is that it provides easy synthetic access to each oxidation state of the thiadiazole, which is essential if tuning of the reduction potential for a specific material application is needed. All heterocycles were characterized by NMR, EA, MS, and X-ray crystallography (see Supporting Information).

The molecular structure of **2a** in the solid state has been previously reported,[14] and the structures of the remaining compounds are reported here. The heterocyclic rings of **2** show slight deviations from planarity, whereas the heterocyclic rings of both **3** and **4** are coplanar to the aromatic carbon backbone. Thiadiazole oxides **2** and **4** show solid-state C−N−S−O dihedral angles between 113° and 128°, and each compound shows similar heterocyclic ring bond lengths. The heterocyclic C−N bond distances for **2**−**4** are ∼1.3 Å, which is consistent with C−N double bond character. Both the C1−C2 and N−S bond lengths are consistent with single bonds resulting in a structure that is more accurately described as a diimine. Crystal packing diagrams of all compounds are included in the Supporting Information. Compounds **2**−**4** stack into columns with overlapping π-systems. Heterocycles **3** pack into parallel stacks with heterocyclic rings overlapping, as opposed to **2** and **4**, which form antiparallel π-stacks, most likely because of dipole−dipole interactions. Intermolecular interactions for the oxides are supported by decomposition temperatures of 316 °C for **4b** compared to 200 °C for **3b**.

(5) (a) Izuhara, D.; Swager, T. M. *J. Am. Chem. Soc.* **2009**, *131*, 17724–17725. (b) Janietz, S.; Barche, J.; Wedel, A.; Sainova, D. *Macromol. Chem. Phys.* **2004**, *205*, 187–198. (c) Moslin, R. M.; Andrew, T. L.; Kooi, S. E.; Swager, T. M. *J. Am. Chem. Soc.* **2009**, *131*, 20–21. (d) Yasuda, T.; Sakai, Y.; Aramaki, S.; Yamamoto, T. *Chem. Mater.* **2005**, *17*, 6060–6068.

(6) (a) Amb, C. M.; Beaujuge, P. M.; Reynolds, J. R. *Adv. Mater.* **2010**, *22*, 724–728. (b) Beaujuge, P. M.; Pisula, W.; Tsao Hoi, N.; Ellinger, S.; Müllen, K.; Reynolds, J. R. *J. Am. Chem. Soc.* **2009**, *131*, 7514–7515. (c) Beaujuge, P. M.; Subbiah, J.; Choudhury, K. R.; Ellinger, S.; McCarley, T. D.; So, F.; Reynolds, J. R. *Chem. Mater.* **2010**, *22*, 2093–2106. (d) Kim, J.-S.; Lu, L.; Sreearunothai, P.; Seeley, A.; Yim, K.-H.; Petrozza, A.; Murphy, C. E.; Beljonne, D.; Cornil, J.; Friend, R. H. *J. Am. Chem. Soc.* **2008**, *130*, 13120–13131. (e) Tsai, J.-H.; Lee, W.-Y.; Chen, W.-C.; Yu, C.-Y.; Hwang, G.-W.; Ting, C. *Chem. Mater.* **2010**, *22*, 3290–3299. (f) Zhang, X.; Steckler, T. T.; Dasari, R. R.; Ohira, S.; Potscavage, W. J., Jr.; Tiwari, S. P.; Coppee, S.; Ellinger, S.; Barlow, S.; Brédas, J.-L.; Kippelen, B.; Reynolds, J. R.; Marder, S. R. *J. Mater. Chem.* **2010**, *20*, 123–134. (g) Zhou, H.; Yang, L.; Xiao, S.; Liu, S.; You, W. *Macromolecules* **2010**, *43*, 811–820.

(7) (a) Bauer, P.; Wietasch, H.; Lindner, S. M.; Thelakkat, M. *Chem. Mater.* **2007**, *19*, 88–94. (b) Fischer, M. K. R.; Kaiser, T. E.; Würthner, F.; Bäuerle, P. *J. Mater. Chem.* **2009**, *19*, 1129–1141. (c) Neuteboom, E. E.; van Hal, P. A.; Janssen, R. A. J. *Chem.—Eur. J.* **2004**, *10*, 3907–3918. (d) Zhang, J.; Hoeben, F. J. M.; Pouderoijen, M. J.; Schenning, A. P. H.; Meijer, E. W.; Schryver, F. C.; De Feyter, S. *Chem.—Eur. J.* **2006**, *12*, 9046–9055.

(8) (a) Gilot, J.; Wienk, M. M.; Janssen, R. A. J. *Adv. Mater.* **2010**, *22*, E67−E71. (b) Ma, C.-Q.; Fonrodona, M.; Schikora, M. C.; Wienk, M. M.; Janssen, R. A. J.; Bäuerle, P. *Adv. Funct. Mater.* **2008**, *18*, 3323–3331. (c) Muller, J. G.; Lupton, J. M.; Feldmann, J.; Lemmer, U.; Scharber, M. C.; Sariciftci, N. S.; Brabec, C. J.; Scherf, U. *Phys. Rev. B: Condens. Matter Mater. Phys.* **2005**, *72*, 195208/195201–195208/195210.

(9) (a) Biniek, L.; Chochos, C. L.; Hadzioannou, G.; Leclerc, N.; Leveque, P.; Heiser, T. *Macromol. Rapid Commun.* **2010**, *31*, 651–656. (b) Coffin, R. C.; Peet, J.; Rogers, J.; Bazan, G. C. *Nat. Chem.* **2009**, *1*, 657–661. (c) Koppe, M.; Egelhaaf, H.-J.; Dennler, G.; Scharber, M. C.; Brabec, C. J.; Schilinsky, P.; Hoth, C. N. *Adv. Funct. Mater.* **2010**, *20*, 338–346.

(10) (a) Biju, P.; Yu, Y. *Tetrahedron Lett.* **2007**, *48*, 5279–5282. (b) Dunn, P. J.; Rees, C. W. *J. Chem. Soc., Perkin Trans. 1* **1989**, 2485–2487.

(11) Algieri, A. A.; Luke, G. M.; Standridge, R. T.; Brown, M.; Partyka, R. A.; Crenshaw, R. R. *J. Med. Chem.* **1982**, *25*, 210–212.

(12) (a) Barton, D. H. R.; Bubb, W. A. *J. Chem. Soc., Perkin Trans. 1* **1977**, 916–923. (b) Daley, S. T. A. K.; Rees, C. W. *J. Chem. Soc., Perkin Trans. 1* **1987**, 207–210. (c) Duan, X.-G.; Duan, X.-L.; Rees, C. W.; Yue, T.-Y. *J. Chem. Soc., Perkin Trans. 1* **1997**, 2597–2601. (d) Mataka, S.; Takahashi, K.; Ishii, S.; Tashiro, M. *J. Chem. Soc., Perkin Trans. 1* **1979**, 2905–2908.

(13) (a) Mirifico, M. V.; Caram, J. A.; Gennaro, A. M.; Cobos, C. J.; Vasini, E. J. *J. Phys. Org. Chem.* **2009**, *22*, 964–970. (b) Svartman, E. L.; Rozas, M. F.; Piro, O. E.; Castellano, E.; Mirifico, M. V. *Synthesis* **2006**, 2313–2318. (c) Wright, J. B. *J. Org. Chem.* **1964**, *29*, 1905–1909.

(14) Arora, S. K. *Acta Crystallogr., Sect. B: Struct. Sci.* **1974**, *B30*, 2923–2925.

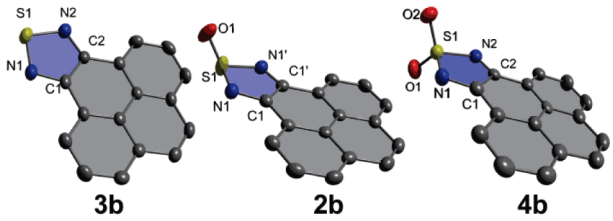

Figure 1. Molecular structures of the pyrenyl series **b** in the solid state (H atoms omitted for clarity; see Supporting Information for details).

The absorption spectra of heterocycles **2**−**4** are shown in Figure 2. PhenSO, **2a**, has a broad $\pi-\pi^*$ transition centered

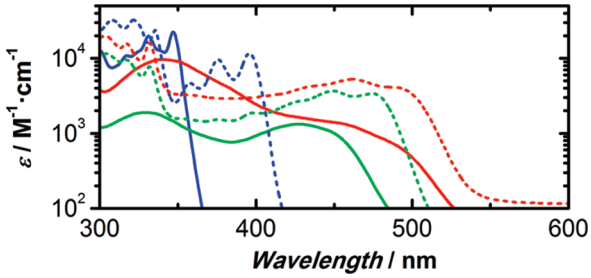

Figure 2. Absorption spectra of compounds **2**−**4** in xylenes. Molar absorptivites of **2a** (green solid), **2b** (green dashed), **3a** (blue solid), **3b** (blue dashed), **4a** (red solid), and **4b** (red dashed).

at 430 nm with a moderate absorptivity of 1300 M^{-1} cm^{-1}. The corresponding peak in PyrSO, **2b**, is red-shifted to 475 nm (ε = 3400 M^{-1} cm^{-1}), as expected by the additional ethylene conjugation. Pyrenyl compounds **2b** and **4b** also show intermolecular interactions in DMF resulting in broad absorption features between 600 and 800 nm (Supporting Information). The optically determined HOMO−LUMO gap is quantified by the absorption onset and two clear trends are evident (Table 1). First, both series **a** and **b** show a red-shift in absorption that correlates with sulfur oxidation state of the thiadiazole heterocycle. The S(II) heterocycles, **3a**,**b**, have the highest energy optical transitions followed by S(IV) heterocycles, **2a**,**b**, and finally S(VI) heterocycles, **4a**,**b**. Second, the pyrenyl systems possess red-shifted absorptions compared to analogous phenanthryl heterocycles (Table 1).

Table 1. Electrochemical and Photophyiscal Properties of **2**−**4**

	$E_{1/2}$,[a] V	k_{et},[b] cm s^{-1}	abs_{onset}, eV (nm)	emission, eV (nm)	E_{LUMO},[c] eV
2a	−1.16	14.3	2.6 (483)		−3.64
2b	−0.88	2.1	2.4 (510)	3.0 (416)	−3.92
3a	−2.07	12.9	3.4 (365)	3.3 (380)	−2.73
3b	−2.08	3.3	3.0 (416)	3.0 (419)	−2.72
4a	−0.64/−1.40	36.8/35.9	2.4 (525)	2.1 (580)	−4.16/−3.40
4b	−0.66/−1.51	2.5/3.7	2.3 (542)	2.2 (553)	−4.18/−3.29

[a] Average of anodic and cathode peak potentials. [b] Calculated using method reported by Nicholson.[15] [c] Calculated using the Ferrocene HOMO level at $-(4.8 + E_{1/2})$ eV.

Normalized fluorescence spectra of heterocycles **2**−**4** in xylenes are summarized in Table 1 and included in the Supporting Information. Expectedly, PyrSO (**3b**) shows a red-shifted emission peak compared to its phenanthryl analogue **3a**. However, $PhenSO_2$ (**4a**) has a red-shifted solution emission compared to $PyrSO_2$ (**4b**), suggesting an intermolecular interaction in xylenes for **4a**. The solid-state emission spectra of heterocycles **2**−**4** are included in the Supporting Information, and all heterocycle emissions are different from solution emissions because they exhibit vibronic bands and are red-shifted. All oxides **2a**,**b** and **4a**,**b** have similar solid-state emission peaks around 610 nm, supporting the role that the oxide(s) play(s) in intermolecular interactions, as supported by the crystal structures. These solid-state emission properties are encouraging for use in D−A polymers for OPV applications because of the enhanced absorption profile and added crystallinity for charge carrier ability.[9a,b,16]

The critical electron-accepting abilities of heterocycles **2**−**4** were assessed by cyclic voltammetry (CV). Both series **a** and **b** display similar electrochemical features, and the discussion below pertains to both phenanthryl and pyrenyl systems. The CVs of **2** and **3** (see Supporting Information) show quasi-reversible redox behavior consistent with the one-electron reduction to the radical anion as assessed by the separation between anodic and cathodic peak potentials. Both dioxides, **4a** and **4b**, show two stepwise one-electron reductions to the radical anion and dianion. As expected, there is a clear trend of redox potential with the heterocyclic sulfur oxidation state. Compounds **3a**, **2a**, and **4a** have their first reduction potentials at −2.07, −0.95 and −0.64 V vs Fc/Fc^+, respectively. Similarly, **3b**, **2b**, and **4b** have their first reduction potentials of −2.08, −0.88 and −0.66 V vs Fc/Fc^+, respectively. Pyrenyl series **b** also shows electrode (glassy carbon) adsorption features, which appear as pre- and postwaves to the main redox peaks in the CV experiments. Despite the high electrolyte concentration, surface adsorption occurs and supports the aggregation behavior observed in the optical measurements. As a comparison, BTD has a reduction potential of −2.12 V and a related P(V)-based phenanthrene at −0.95 V under the same electrochemical conditions.[17] Interestingly, the electron transfer rates of the phenanthryl series **a** were approximately 1 order of magnitude faster than those of the pyrenyl analogues (Table 1).

The tunable reduction potentials, by simply varying the S oxidation state, highlight the utility of these compounds as candidate *n*-type functional monomers. The oxidation tuning can be exploited in the design of tailored low band gap D−A copolymers with E_{LUMO} values near the ideal −3.9 eV for

(15) Nicholson, R. S. *Anal. Chem.* **1965**, *37*, 1351–1355.
(16) Ong, B. S.; Wu, Y.; Liu, P.; Gardner, S. *J. Am. Chem. Soc.* **2004**, *126*, 3378–3379.
(17) Linder, T.; Sutherland, T. C.; Baumgartner, T. *Chem.—Eur. J.* **2010**, *16*, 7101–7105.

OPV applications,[18] assuming a band gap of 1.5 eV, in efforts to achieve 10% OPV efficiency.[18]

Heterocycles **2**−**4** were subjected to DFT calculations[19] (B3LYP-6-31G+d,p) to assess the orbitals involved in the redox reactions, as well as their energies (Figure 3). The

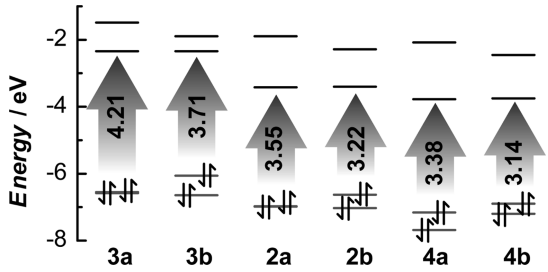

Figure 3. Calculated FMO energy levels of compounds **2**−**4**.

trend in LUMO energy levels mirror the results found by the electrochemically determined LUMO energy levels. A lowering of the LUMO energy level is found when comparing heterocycles S(II) **3** with S(IV) **2** and S(VI) **4**, whereas the backbone has little influence on the LUMO. Compounds **3a** and **2a** also contain nearly degenerate HOMO energy levels, whereas **3b** and **2b** have higher energy, discrete occupied FMOs because of the added conjugation. Again, the higher HOMOs of series **b**, in conjunction with similar LUMO energies, results in the pyrenyl systems having smaller HOMO−LUMO energy gaps, which is consistent with the observed absorption onsets. The energy-optimized structures of **2**−**4** are nearly identical to the experimental crystal structures lending support to the calculated geometries. The HOMO and HOMO-1 are nearly degenerate for **2a** with electron density confined to the heterocyclic ring in the HOMO-1 and localized on the phenanthrene backbone for the HOMO. In **2b**, the HOMO and HOMO-1 energies are split. The **2b** HOMO shares features with the HOMO-1 of **2a**, and the HOMO-1 of **2b** is similar to the HOMO of **2a**. The additional ethylene bridge in **2b** raises the HOMO energy level. Note the LUMOs of **2b** and **2a** have nearly identical coefficients and energies because the ethylene bridge does not play a role (see Supporting Information). Both the electrochemical reduction (E_{LUMO}) and the absorption onset (HOMO−LUMO gap) are consistent with the calculations, suggesting the DFT results correctly describe the FMOs in solution. The FMOs of **3** and **4** are similar with the LUMOs confined to the heterocyclic ring and are included in the Supporting Information.

To further assess the synthetic potential of these building blocks as monomers for polymerizations the 2,7-dibromo-PhenSO, **5**, accessible in a similar protocol via the dibromophenanthrene quinone, was representatively subjected to a Stille cross-coupling reaction to provide the bis(aniline) species **6** (Scheme 2). Due to the extended π system and its

Scheme 2. Cross-Coupling of Dibromo-thiadiazole(oxide) **5**

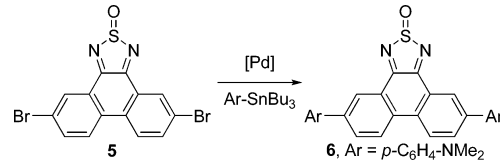

D−A character, **6** shows a red-shifted emission at 595 nm (cf. 538 nm for **2a** in CH_2Cl_2). The absorption maximum of **6**, on the other hand, remains the same as **2a** at 430 nm. These observations are in line with the D−A nature of **6**.

In summary, we have synthesized a series of thiadiazole heterocycles that show strong electron-accepting characteristics, particularly for the S(IV) and S(VI) congeners, which are supported by DFT, absorption spectroscopy, and electrochemical measurements. The results emphasize the high value of these building blocks for the generation of *n*-type conjugated organic materials.

Acknowledgment. The authors thank NSERC of Canada and the Institute for Sustainable Energy, Environment, and Economy.

Supporting Information Available: Synthetic details and NMR spectra, X-ray crystallographic details, absorption, fluorescence and excitation spectra, CVs, TGAs, FMOs, and computational details. This material is available free of charge via the Internet at http://pubs.acs.org.

OL1018213

(18) (a) Scharber, M. C.; Muehlbacher, D.; Koppe, M.; Denk, P.; Waldauf, C.; Heeger, A. J.; Brabec, C. J. *Adv. Mater.* **2006**, *18*, 789–794. (b) Zhou, H.; Yang, L.; Stoneking, S.; You, W. *ACS Appl. Mater. Interfaces* **2010**, *2*, 1377–1383.

(19) Frisch, M. J. et al. *Gaussian 03, Revision E.01*; Gaussian, Inc.: Wallingford, CT, 2004.